ISSN 2176-5480

22nd International Congress of Mechanical Engineering (COBEM 2013)
November 3-7, 2013, Ribeirão Preto, SP, Brazil

NUMERICAL DETERMINATION OF DISCHARGE COEFFICIENTS OF ORIFICE PLATES AND NOZZLES

F. H. J. Imada
F. Saltara
J. L. Baliño
Universidade de São Paulo, Departamento de Engenharia Mecânica, São Paulo, Brazil
fabiano.imada@usp.br

Abstract. *Differential pressure devices such as orifice plates and nozzles are extensively applied in several industries in order to estimate the mass flow rate running through a conduit by correlating the measured pressure loss and the mass flow rate. The discharge coefficient C_D relates the actual mass flow rate to the theoretical flow rate through the device. The ISO 5167:2003 Standard (ISO, 2003) suggests equations for calculating the C_D of orifice plates, nozzles and Venturi tubes inserted in circular cross-section ducts. In this work, the commercial finite-volume based code FLUENT is used to evaluate the C_D of orifice plates and long radius nozzles with diameters ratio $\beta = 0.50$ in the Reynolds range $15,000 - 500,000$. Incompressible steady-state analyses are conducted in three-dimensional domains discretized with unstructured meshes. Grid convergence studies are conducted evaluating the Grid Convergence Index (GCI) through the procedure suggested by Roache (1997). Pressure-velocity coupling is calculated via Pressure Implicit with Splitting of Operators (PISO) algorithm; pressure and velocities are resolved through a staggered grid scheme. All other variables are interpolated via Second-order Upwind method. The results for two turbulence models - Realizable $k - \epsilon$ and Shear Stress Transport (SST) $k - \omega$ - are obtained. The calculated values of discharge coefficients are in good agreement with the ISO Standard.*

Keywords: *flow measurement, differential pressure devices, orifice plate, nozzle, Computational Fluid Dynamics.*

1. INTRODUCTION

Measuring the mass flowrate of a fluid running through a conduit is a recurrent need in several industrial processes, such as natural gas transport ducts and fluid feeding systems in petrochemical, steel mill and ethanol distillery industries. Among the available flow metering methods, pressure differential-based devices are extensively applied due to their design and operational simplicity and low cost maintenance. Examples of pressure differential meters are orifice plates, nozzles and Venturi tubes.

By this method, the insertion of a physical barrier perpendicular to the tube axis leads to a flow area reduction causing a local fluid acceleration and therefore a pressure drop. Considering an idealized incompressible flow, the pressure drop can be related to the mass flowrate of the fluid (Fox *et al.*, 2004). However, inertial and viscous effects need to be accounted for, which is accomplished by means of the introduction of a correction factor, namely the discharge coefficient C_D.

The ISO Standard 5167:2003 (ISO, 2003) specifies the geometry design, installation and operation conditions of such devices when a single phase fluid flows in a circular duct. This ISO Standard also establishes the general principles and methods of measurement and calculation of the mass flowrate and the C_D under different conditions (flow Reynolds number, diameters ratio β, pressure tappings location and presence of upstream tube fittings).

The influence of operational conditions in the flow field development through differential pressure devices has been experimentally studied by several researchers. Morrison *et al.* (1990) evaluated the influence of β ratio (ratio between the meter orifice d and the tube diameter D), swirl (flow axial rotation) upstream the device and Reynolds number on wall pressure distribution in flows through orifice meters. Morrison *et al.* (1992) studied the dependence of the orifice discharge coefficient on the upstream velocity profile. Using a 3D laser Doppler anemometer system, Morrison *et al.* (1993) visualized the mean velocity and turbulent kinetic energy fields in the vicinity of a $\beta = 0.50$ orifice flowmeter. Morrow *et al.* (1991) also evaluated the sensitivity of the the discharge coefficient of orifice plates under different upstream velocity profiles.

Details of the flow around the metering device have also been investigated by means of Computational Fluid Dynamics. Erdal and Andersson (1997) studied the influence of turbulence effects through the Standard $k - \epsilon$ model (Launder and Spalding, 1974) and a modified one on pressure distribution in the upstream and downstream regions of orifices. They used a 2D axisymmetric domain and compared the simulated results to experiments. Lee *et al.* (2006) applied the Finite Volume Method to simulate critical flow of Hydrogen through convergent-divergent nozzles at high pressures. A real-gas equation of state was used to adequately relate the fluid properties dependence on pressure and temperature conditions. The calculated results of pressure distribution, flow velocity and meter discharge coefficient were compared to experimental data.

ISSN 2176-5480

Eiamsa-ard *et al.* (2008) performed simulations of compressible flows through orifice plates with three different β ratios. They compared results of axial velocity and pressure gradient results for three interpolation schemes (First-order Upwind, Second-order Upwind and Quadratic Upstream Interpolation for Convective Kinetics - QUICK) and two turbulence models (Standard $k-\epsilon$ and Reynolds Stress Model (Launder, 1989)) to experimental data. The influence of the orifice plate thickness on the discharge coefficient was numerically investigated by Singh *et al.* (2010). They evaluated the C_D for four different β ratios using 2D axisymmetric domains applying the Semi-Implicit Method for Pressure-Linked Equations (SIMPLE) algorithm (Patankar and Spalding, 1972) for calculating pressure-velocity coupling. Also applying the SIMPLE algorithm, Oliveira *et al.* (2010) simulated water flows through orifice plates suggesting a numerical procedure for constructing the metering calibration curve for different Reynolds number, β ratio and pressure tappings position. They also applied the Reynolds Stress Model in order to account for turbulence effects using a staggered grid scheme (Versteeg and Malalasekera, 1995). The calibration curve obtained was compared to own experimental data.

Arun *et al.* (2010) calculated single phase flows of non-Newtonian fluids through orifice plates. Three β ratios were investigated under flow conditions in the range of Reynolds $100-100,000$ for different concentrations of the non-Newtonian fluid. They identified an exponential increase of the discharge coefficient in the range of Re $100-10,000$ and a settling around $C_D = 0.60$ with further increase of Reynolds number. Hollingshead *et al.* (2011) evaluated the discharge coefficient of orifice plates, Venturi tubes, V-cones and wedges flowmeters for flows in the range of Reynolds $100-1,000,000$ comparing the numerical results with experimental data. Steady state three-dimensional simulations of incompressible flows were conducted with the Realizable $k-\epsilon$ model (Shih *et al.*, 1995) being used for modeling turbulence effects. Pressure-velocity coupling was resolved by the SIMPLE algorithm. They applied the Grid Convergence Index (GCI) (Roache, 1997) to evaluate grid-related uncertainties. They also proposed correction factors for the C_D of each meter according to the flow Reynolds number. Shah *et al.* (2012) conducted three-dimensional simulations of compressible and incompressible flows through orifice plates for different β ratios, tube diameters and inlet velocities. The standard $k-\epsilon$ model was applied with the pressure-velocity coupling being calculated by the SIMPLE scheme. Second-order Upwind algorithm was used for interpolating the flow variables. Results of pressure distributions, turbulent kinetic energy fields and axial velocities ere compared to experimental data available in the literature.

In this work, the finite volume-based code FLUENT was applied to simulate incompressible flows in the Reynolds range $15,000-500,000$ through orifice plates and long radius nozzles. Mesh uncertainty was evaluated through the GCI criteria. The calculated discharge coefficients obtained by means of two turbulence models were compared to the expected values from the ISO Standard 5167:2003 equations (ISO, 2003).

2. SIMULATIONS

2.1 Governing equations

The calculation of steady state incompressible flow is accomplished by solving the mass and momentum conservation equations given as:

$$\rho\frac{\partial U_i}{\partial x_i} = 0 \tag{1}$$

$$\frac{\partial}{\partial x_j}\left(\rho U_i U_j\right) = \frac{\partial P}{\partial x_i} + \frac{\partial \tau_{ij}}{\partial x_j} + \rho g_i + \frac{\partial}{\partial x_j}\left(-\overline{\rho u_i u_j}\right) \tag{2}$$

where ρ is fluid density, U_i represents the flow mean velocity components, x_i the spatial coordinates, P is the mean pressure, τ_{ij} is the mean viscous stress tensor, g_i being the gravitational acceleration and the last term $-\overline{\rho u_i u_j}$ is the Reynolds stress tensor which needs to be modeled for closuring the problem. In this work, the Realizable $k-\epsilon$ turbulence model proposed by Shih *et al.* (1995) and the Shear-Stress Transport (SST) $k-\omega$ model developed by Menter (1994) were used for the closure solution for the above equation set.

The Realizable $k-\epsilon$ model is a two-equation formulation which determines the turbulent length and time scales by solving two transport equations: one related to the turbulent kinetic energy k and its dissipation rate ϵ. The SST $k-\omega$ model is also classified as a two-equation model which blends the $k-\epsilon$ approach applied in the outer region of the boundary layer while solving the k equation and an additional transport equation for the turbulence kinetic energy specific dissipation rate ω in the inner part of the boundary layer.

2.2 Geometry details

Geometries of an orifice plate and a long radius nozzle with diameters ratio $\beta = d/D = 0.50$ were elaborated with nominal tube diameter $D = 2.0\,in$. Design details were obtained from ISO (2003). Upstream the meter, a straight tube length $L_{up} = 30\,D$ is positioned and a straight length $L_{down} = 20\,D$ downstream the device is also modeled, as shown in Fig. 1.

ISSN 2176-5480

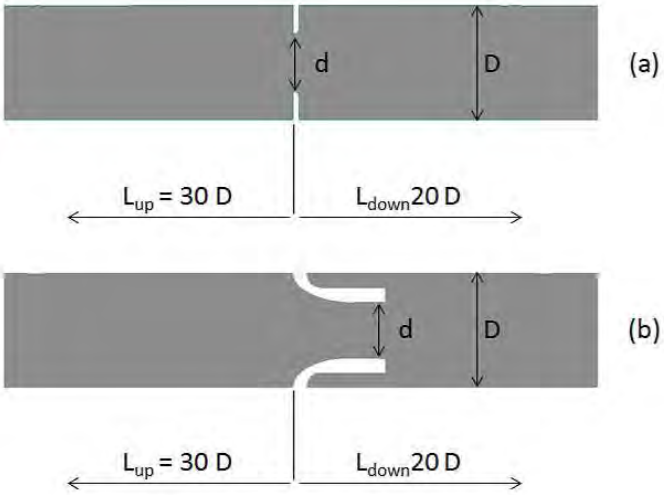

Figure 1. Computational domain: (a) orifice plate and (b) long radius nozzle.

2.3 Grid resolution

The computational domains were discretized with unstructured polyhedral meshes with a prismatic elements layer in the region near the walls in order to adequately capture the flow gradients in such areas. Figure 2 shows a longitudinal plane cut of the grids around both flowmeters under study.

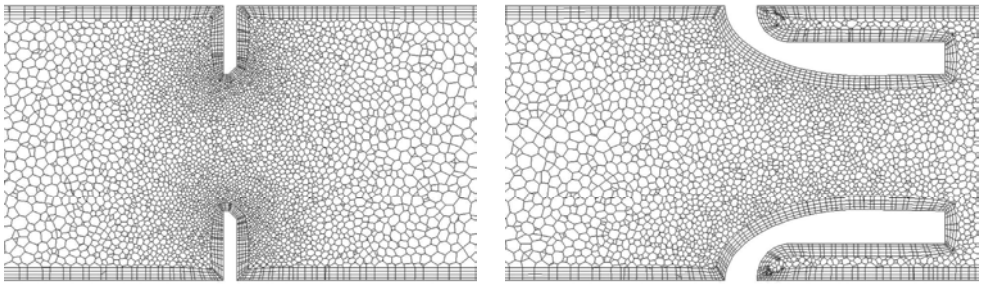

Figure 2. Mesh around (a) orifice plate; (b) long radius nozzle - $Re = 150,000$.

Grid uncertainty was verified by means of the GCI criteria following the procedure suggested by Roache (1997). Through this method, for each condition simulated, three meshes with different discretization resolutions were elaborated and used in calculation. The meshes were elaborated in a way that the coarser mesh, here defined as *Coarse Mesh*, presents a characteristic element size 1.2 larger the next level mesh, defined as *Base Mesh*, which also presents an element size 1.2 larger than the element of the finer mesh, named *Fine Mesh*. Comparing the simulation results obtained with the three grid levels, the GCI procedure provides an estimative of the uncertainty related to the spatial discretization of the *Fine Mesh*.

2.4 Boundary conditions and solution procedure

Steady state simulations of incompressible fluid flow were performed at Reynolds 15,000, 50,000, 150,000 and 500,000 conditions. For each condition, a prior simulation using a straight tube with length $L = 300\,D$ was performed in order to obtain developed profiles of velocity and turbulent quantities at the tube outlet. Such developed profiles were defined as inlet conditions upstream the devices. Static atmospheric pressure is defined at the tube exit downstream the flowmeters. Water was used as operational fluid with density $\rho = 998.2\,kg/m^3$ and dynamic viscosity $\mu = 0.001\,Pa.s$. Wall functions are used to provide turbulence boundary conditions at smooth walls which experience the no slip condition.

Pressure-velocity coupling was calculated via the Pressure Implicit with Splitting of Operators (PISO) algorithm (Issa, 1985). Pressure and velocities values were interpolated by means of a staggered grid method (Ferziger and Peric, 2002). All variables were interpolated with Second-order Upwind algorithm (Ferziger and Peric, 2002).

The convergence criteria was adopted as the decay of four orders of magnitude of the normalized residuals and the settling of flow measures such as outlet mass flow rate, mean velocity at the exit and mean wall shear stress.

ISSN 2176-5480

3. RESULTS

For the simulations of the flow through orifice plates, absolute pressure values were obtained at positions corresponding to D and $D/2$ pressure tappings configuration, i.e., the spacing l_1 of the upstream pressure tapping is nominally equal to D while the spacing l_2 of the downstream pressure tapping is nominally equal to $0.5D$. Both l_1 and l_2 spacings are measured from the upstream face of the orifice plate. The same pressure tappings configuration is applied the long radius nozzles, with the difference that the l_1 and l_2 spacings are measured from the inlet face of the nozzle.

The pressure drop at the flowmeter is then calculated as $\Delta P = P_1 - P_2$, where P_1 is the upstream absolute pressure and P_2 is the downstream absolute pressure. Additionally to the pressure difference, results of mass flow rate q_m at tube outlet are evaluated and the device discharge coefficient is then calculated as:

$$C_D = \frac{4q_m\sqrt{1-\beta^4}}{\pi d^2\sqrt{2\Delta P\rho}} \tag{3}$$

ISO (2003) provides equations for the calculation of the discharge coefficient as a function of Reynolds number, β ratio, pressure tappings and fluid properties. The values estimated by these equations, named here as *ISO values*, were compared to the ones obtained with the Realizable $k-\epsilon$ and with the SST $k-\omega$ turbulence models.

Figure 3 shows the *ISO values* and the results of the *Fine Mesh* obtained with the two turbulence models applied for the orifice plate simulations. The uncertainty of 0.5% related to the ISO equation is shown in its plot. The pressure drop through the orifice is mainly caused by the abrupt deflection of the flow which gives rise to the phenomenon known as *vena contracta*, i.e., a region where the fluid stream presents a minimum diameter (lower than the orifice diameter as shown in Fig. 4) and a maximum velocity. Both turbulence models are able to capture this behaviour, but present an under-estimation of the pressure drop through the orifice which leads to a higher calculated C_D when compared to the expected values from the ISO Standard. The SST $k-\omega$ model performs better than the Realizable $k-\epsilon$ formulation, which presents the largest deviation (4.92% from *ISO values*). Maximum mesh discretization uncertainty was 4.09%.

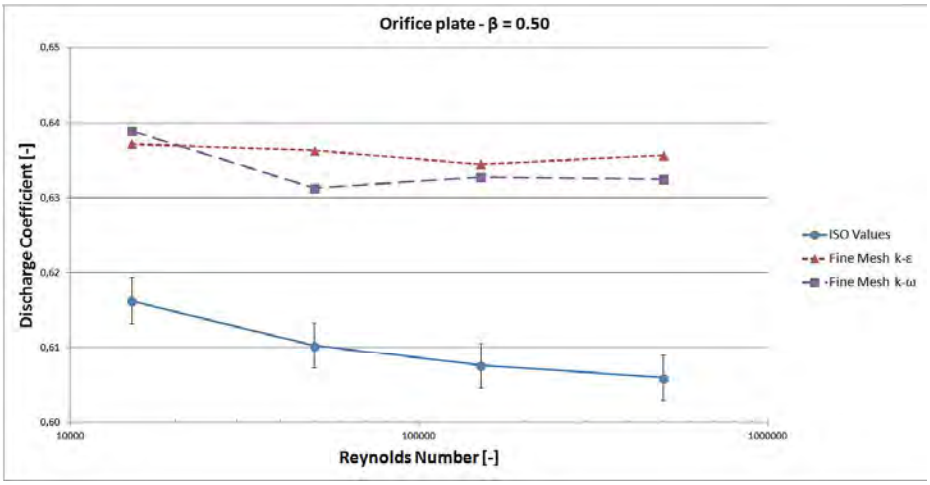

Figure 3. Discharge coefficients of orifice plate.

The results concerning the long radius nozzles can be observed in Fig. 5 which shows the *ISO values* and the results obtained with the *Fine Mesh* for the two turbulence models. The pressure drop in nozzles is mainly caused by viscous dissipation at the device surface and is well captured by both turbulence models. The simulated results of C_D are slightly under-estimated (maximum difference of -0.98%) when compared to the calculated values from ISO equation but within its uncertainty of 2.0%. The maximum grid uncertainty achieved was 0.60%.

4. CONCLUDING REMARKS

Incompressible flows through an orifice plate and a long radius nozzle with $\beta = 0.50$ at Reynolds range $15,000 - 500,000$ were simulated with the application of the Realizable $k-\epsilon$ and the SST $k-\omega$ turbulence models. The obtained results of discharge coefficient with both models were compared to values expected from the ISO 5167:2003 Standard equations. The simulated C_D of orifice plates were over-estimated (maximum error of 4.92%) by both formulations with the $k-\omega$ model showing slightly better agreement. The predominance of viscous effects in the pressure drop through the nozzles was satisfactory captured with the two turbulence models, presenting under-estimated results of C_D within a 1.0% margin from the ISO Standard expected values.

ISSN 2176-5480

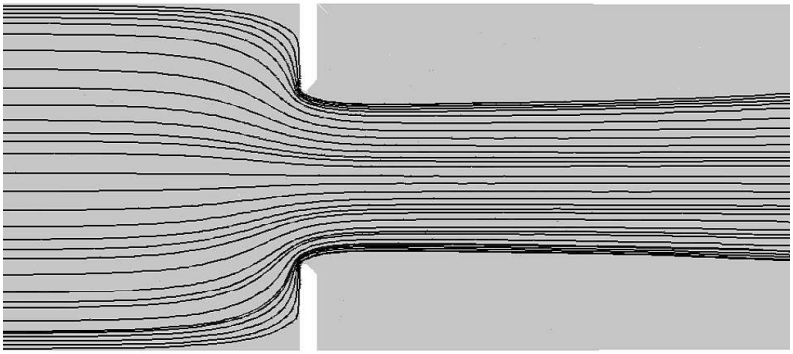

Figure 4. Flow streamlines through orifice plate.

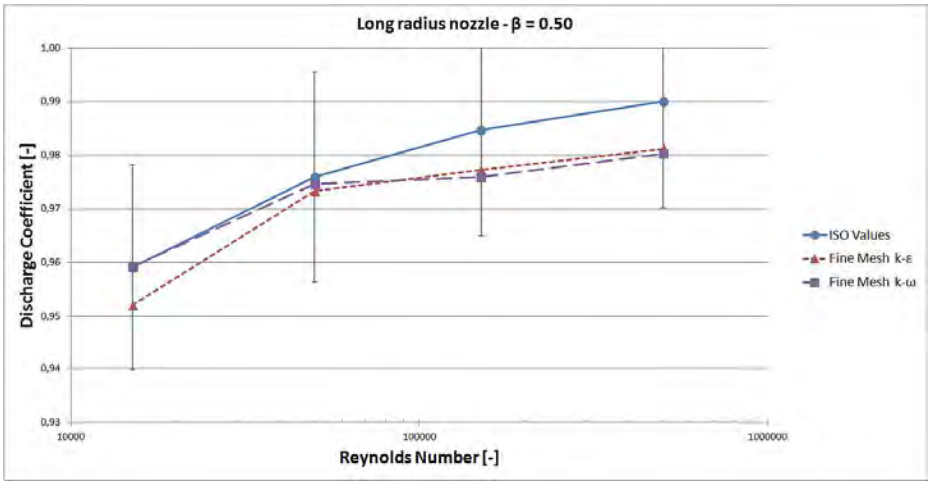

Figure 5. Discharge coefficients of long radius nozzle.

5. ACKNOWLEDGEMENTS

This work was granted by *Petróleo Brasileiro S.A.* (Petrobras). The authors wish to thank to *Agência Nacional do Petróleo* (ANP) and *Conselho Nacional de Desenvolvimento Científico e Tecnológico* (CNPq).

6. REFERENCES

Arun, N., Malavarayan, S. and Kaushik, M., 2010. "Cfd analysis on discharge coefficient during non-newtonian flows through orifice meter". *International Journal of Engineering Science and Technology*, Vol. 2 (7), pp. 3151–3164.

Eiamsa-ard, S., Ridluan, A., Somsavysin, P. and Promvonge, P., 2008. "Numerical investigation of turbulent flow through a circular orifice". *KMITL Science Journal*, Vol. 8, pp. 43–50.

Erdal, A. and Andersson, I., 1997. "Numerical aspects of flow computation through orifices". *Flow Measurement and Instrumentation*, Vol. 8, pp. 27–37.

Ferziger, J.H. and Peric, M., 2002. *Computational methods for fluid dynamics*. Springer.

Fox, R.W., McDonald, A.T. and Pritchard, P.J., 2004. *Introduction to fluid mechanics*. John Wiley & Sons, Inc.

Hollingshead, C., Johnson, M., Barfuss, S. and Spall, R., 2011. "Discharge coefficient performance of venturi, standard concentric orifice plate, v-cone and wedge flow meters at low reynolds numbers". *Journal of Petroleum Science & Engineering*, Vol. 78, pp. 559–566.

ISO, 2003. "Iso standard 5167 - measurement of fluid flow by means of pressure differential devices inserted in circular cross-section conduits running full".

Issa, R.I., 1985. "Solution of the implicitly discretised fluid flow equations by operator-splitting". *Journal of Computa-*

ISSN 2176-5480

tional Physics, Vol. 62, pp. 40–65.

Launder, B.E., 1989. "Second-moment closure: present and future". *International Journal of Heat and Fluid Flow*, Vol. 10, pp. 282–300.

Launder, B.E. and Spalding, D.B., 1974. "The numerical computation of turbulent flows". *Computer Methods in Applied Mechanics and Engineering*, Vol. 3, pp. 269–289.

Lee, J., Kim, H., Park, K., Setoguchi, T. and Matsuo, S., 2006. "Cfd prediction of the critical nozzle flow of high-pressure hydrogen gas". In *Proceedings of the 3rd BSME-ASME International Conference on Thermal Engineering*.

Menter, F.R., 1994. "Two-equation eddy-viscosity turbulence models for engineering applications". *AIAA Journal*, Vol. 32, pp. 1598–1605.

Morrison, G.L., DeOtte, R.E., Moen, M., Hall, K.R. and Holste, J.C., 1990. "Beta ratio, swirl and reynolds number dependence of wall pressure in orifice flowmeters". *Flow Measurement and Instrumentation*, Vol. 1, pp. 269–277.

Morrison, G.L., DeOtte, R.E., Nail, G.H. and Panak, D.L., 1993. "Mean velocity and turbulence fields inside a beta = 0.50 orifice meter". *AIChE Journal*, Vol. 39, pp. 745–756.

Morrison, G.L., R. E. DeOtte, J. and Beam, E.J., 1992. "Installation effects upon orifice flowmeters". *Flow Measurement and Instrumentation*, Vol. 3, pp. 89–93.

Morrow, T.B., Park, J.T. and McKee, R.J., 1991. "Determination of installation effects for a 100 mm orifice meter using a sliding vane technique". *Flow Measurement and Instrumentation*, Vol. 2, pp. 14–20.

Oliveira, N., Vieira, L. and Damasceno, J., 2010. "Numerical methodology for orifice meter calibration". *Materials Science Forum*, Vol. 660-661, pp. 531–536.

Patankar, S.V. and Spalding, D.B., 1972. "A calculation procedure for heat, mass and momentum transfer in three-dimensional parabpara flows". *International Journal of Heat and Mass Transfer*, Vol. 15, pp. 1787–1806.

Roache, P.J., 1997. "Quantification of uncertainty in computacional fluid dynamics". *Annual Review of Fluid Mechanics*, Vol. 29, pp. 123–160.

Shah, M.S., Joshi, J.B., Kalsi, A.S., Prasad, C. and Shukla, D.S., 2012. "Analysis of flow through an orifice meter - cfd simulation". *Chemical Engineering Science*, Vol. 71, pp. 300–309.

Shih, T.H., Liou, W.W., Shabbir, A., Yang, Z. and Zhu, J., 1995. "A new k-epsilon eddy-viscosity model for high reynolds number turbulent flows". *Computers Fluids*, Vol. 24, pp. 227–238.

Singh, R.K., Singh, S.N. and Seshandri, V., 2010. "Performance evaluation of orifice plate assemblies under non-standard conditions using cfd". *Indian Journal of Engineering and Materials Sciences*, Vol. 17, pp. 397–406.

Versteeg, H.K. and Malalasekera, W., 1995. *An introduction to computational fluid dynamics - The finite volume method*. Longman Scientific & Technical.

7. RESPONSIBILITY NOTICE

The authors are the only responsible for the printed material included in this paper.